

P348 in Numbers

B. Vasilishin

Abstract

A short description of the P348 sub-detectors is given.

Contents

1	Experimental Setup	2
2	ECAL	4
3	Vacuum vessel	4
4	Hadronic calorimeter	5
5	Straw chamber	6
6	Sc counters, Veto counters and Sc hodoscopes	6
7	BGO	6
8	Summary	7

1 Experimental Setup

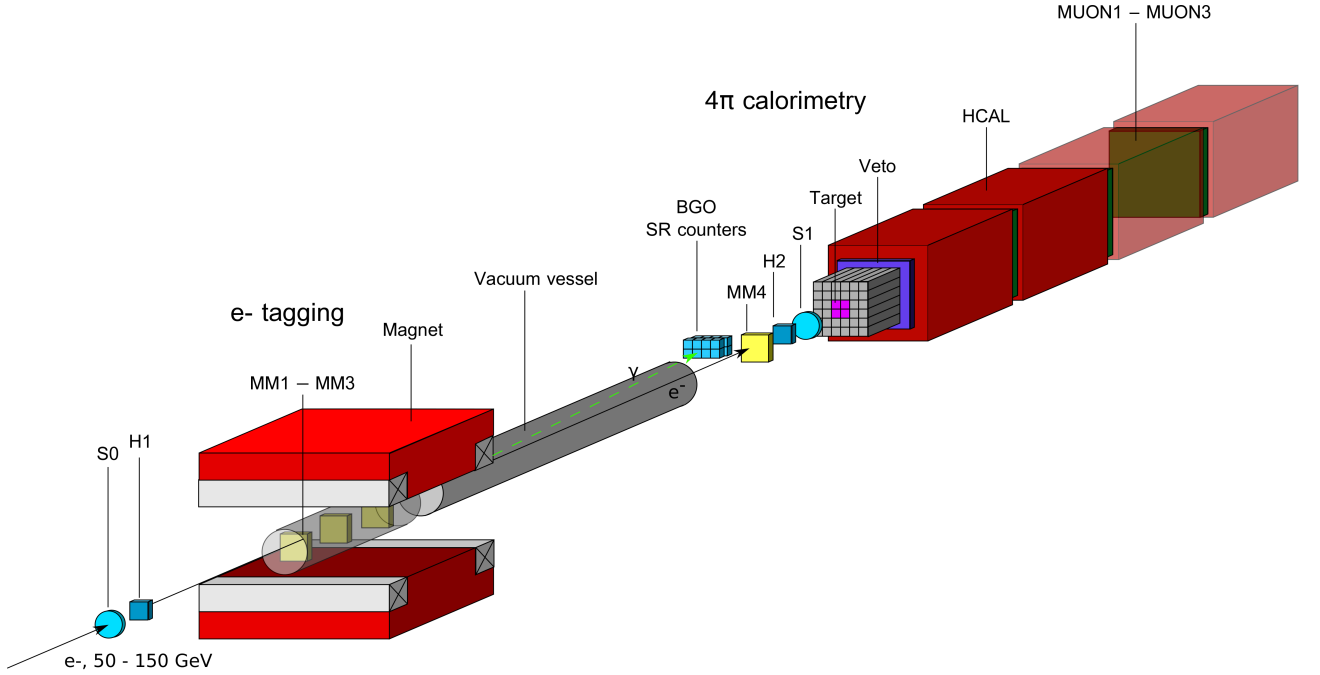


Figure 1: Experimental setup

The experimental setup designed to search for the $A' \rightarrow \text{invisible}$ decays is schematically shown in Fig. 1. The detector is equipped with a low material budget tracker, 4 Micromegas (MM) and 4 straw tubes chambers (SC). The 3 MM chambers were assembled inside vacuum pipe of 159 mm in diameter and inserted inside the 1.5 T magnet upstream of the setup. The straw chambers, with the straw diameter of 6 mm (2 SC) and 2 mm (2 SC) were delivered for tests outside magnetic field. Three scintillation counter S0, S1, S2 were used for beam definition. The setup also uses high density shashlik electromagnetic calorimeter ECAL to detect e^- primary interactions, high efficiency veto counter Veto, two scintillating hodoscope H1, H2 and a hermetic hadron calorimeter HCAL located at the downstream end of the setup in order to detect all final state products from the primary reaction $e^- Z \rightarrow e^- Z A'$. The 15 m long vacuum vessel between the magnet and the ECAL was installed to avoid absorption of the synchrotron radiation photon detected at the downstream end of the vessel by the array of 8 BGO crystals.

The method of the search is the following. The incident electron energy absorption in the ECAL is accompanied by the emission of bremsstrahlung A's in the reaction of electrons scattering on nuclei, due to the $\gamma - A$ mixing:

$$e^- Z \rightarrow e^- Z A'. \quad (1)$$

The reaction (1) typically occurs in the first few radiation length (X_0) of the calorimeter. The part of the primary beam energy is deposited in the ECAL, while the remaining fraction of the total energy is transmitted by light dark matter decay particles χ through the rest of the detector. The χ penetrates the ECAL, Veto and the HCAL without interactions resulting in the missing-energy signature in the detector. The occurrence of $A \rightarrow \text{invisible}$ decays produced in $e^- Z$ interactions would appear as an excess of events with a single e-m showers in the ECAL1, and zero energy deposition in the rest of the detector, above those expected from the background sources. The signal candidate events have the signature:

$$S_{A'} = H1 \times H2 \times ECAL(E_{ECAL} < E_0) \times \overline{Veto} \times \overline{HCAL}, \quad (2)$$

and should satisfy the following selection criteria:

1. The starting point of EM – showers in the ECAL should be localized within a few first X_0 s.
2. The lateral and longitudinal shapes of the shower in the ECAL are consistent with an electromagnetic one.
3. The fraction of the total energy deposition in the ECAL is $f \lesssim 0.5$.
4. No energy deposition in the Veto and HCAL.

One of the main background sources in the experiment is related to the possible presence of the low-energy tail in the energy distribution of beam electrons. This tail is caused by the electron interactions with a passive material, e.g. as entrance windows of the beam lines, residual gas, etc... Another source of low energy electrons is due to the pion or muon decays in flight in the beam line. The uncertainties arising from the lack of knowledge of the dead material composition in the beam line are potentially the largest source of systematic uncertainty in accurate calculations of the fraction and energy distribution of these events. Hence, the sensitivity of the experiment could be determined by the presence of such electrons in the beam, unless one takes special measures to suppress this background. To reject these background sources at high energies by using standard techniques, e.g. threshold Cerenkov counters, is practically impossible.

To improve the primary high energy electrons selection and additionally suppress back- ground from the possible presence of low energy electrons in the beam typically with energy $E_e \lesssim 0.5E_0$ (E_0 – beam energy), one use a high energy e^- -tagging system utilizing the synchrotron radiation (SR) from high energy electrons in a dipole magnet. The basic idea is that, since the critical SR photon energy is $(\hbar\omega)_\gamma^c \propto E_0^3$ the low energy electrons in the beam could be rejected by using, e.g. the cut on $E_\gamma > 0.3(\hbar\omega)_\gamma^c$ in a gamma-ray detector, here it's BGO(read more 7).

2 ECAL

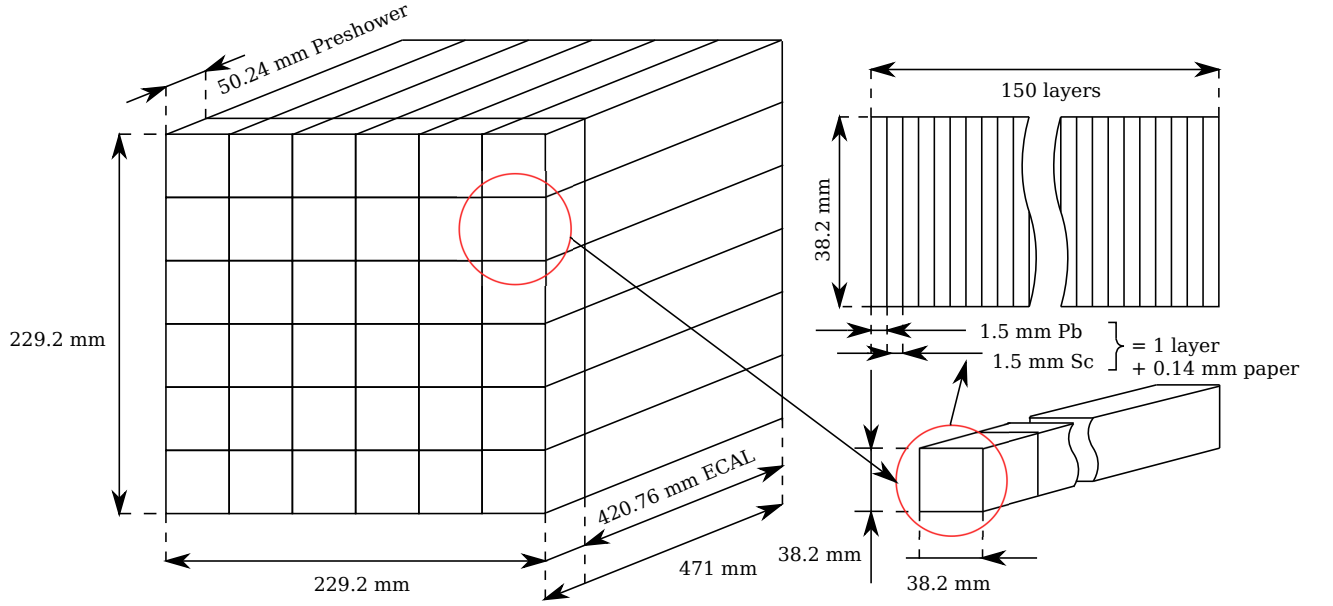


Figure 2: Electromagnetic calorimeter

The electromagnetic calorimeter shown in Fig. 2 is the shashlik type detector designed for energy measurements, shower profile measurements, e/π separation and it's a matrix of 6×6 cells, each with dimensions $38.2 \times 38.2 \times 471 \text{ mm}^3$. Each cell is $(1.50 \text{ mm Pb} + 0.14 \text{ mm paper} + 1.50 \text{ mm Sc}) \times 150$ layers or 40 radiation length (X_0) and is longitudinally subdivided at preshower section of 16 layers ($\sim 4.27X_0$) and the rest 134 layers ($\sim 35.73X_0$) ECAL part. This is done in order to improve the e/π rejection factor the calorimeter each module is subdivided at two, preshower and calorimetry, parts.

The important characteristic feature of the ECAL is that the WLS fibers are inserted in a spiral in order to avoid energy leak through them. Timing and energy deposition information from each PS/ECAL module is digitized for each event.

The short summary of ECAL's characteristics is presented in Table 1.

3 Vacuum vessel

The vacuum vessel is a tank of 26 cm in diameter and about 15 m length. The volume is evacuated to the pressure below 10^{-3} mbar, to minimize SR photon absorption and secondary hadronic interactions in air. The in- and output flanges made of thin Mylar layers, about 20 mg/cm^2 .

4 Hadronic calorimeter

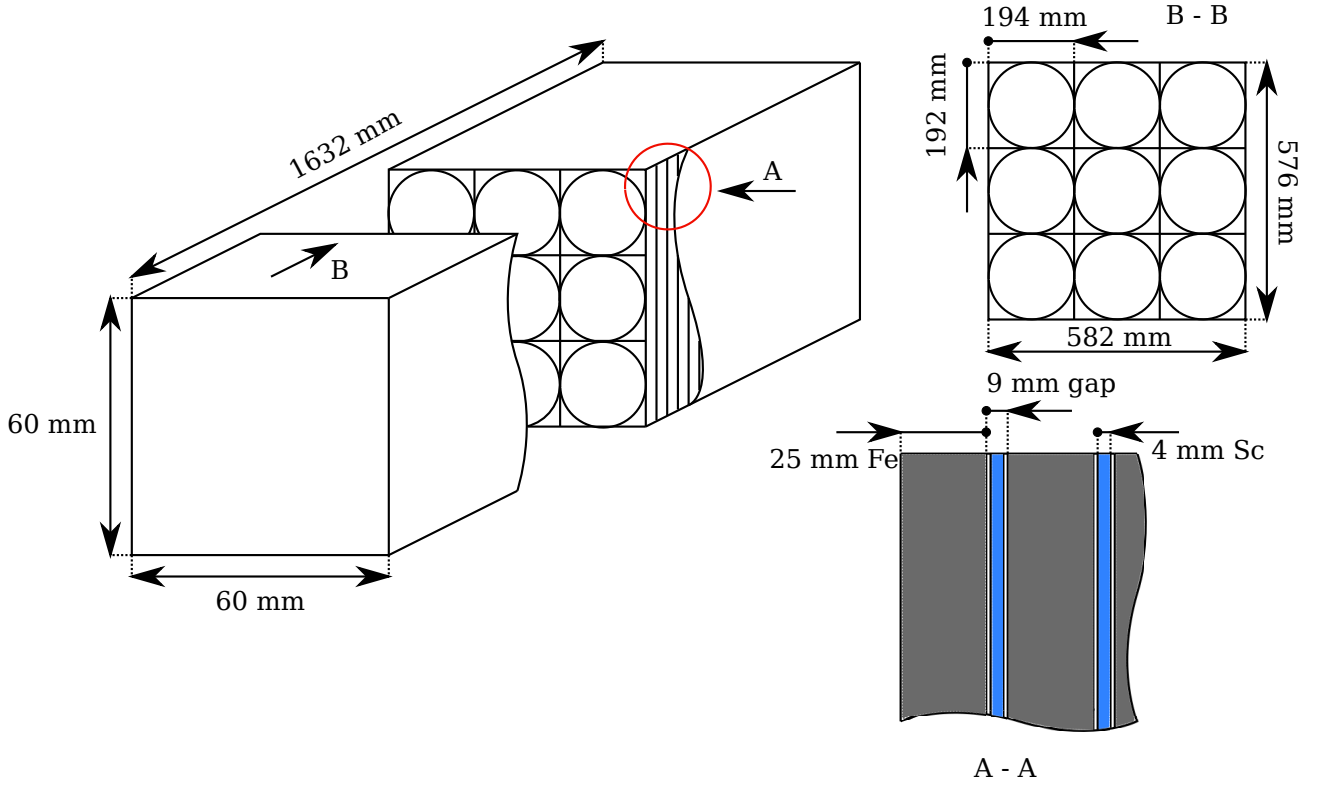


Figure 3: Hadronic calorimeter

Hadronic calorimeter consists of 4 modules (one module shown at Fig. 4 and it's used for secondary energy detection (π , p , n)). Each module is a matrix of 3×3 cells. Each cell is a sandwich of alternating layers of Fe and scintillator plates with thicknesses of 25 mm and 4 mm, respectively, and with a lateral size $194 \times 192 \text{ mm}^2$. There is a gap of 7 mm between two Fe plates, so the total length of one layer is 32 mm. Each cell consists of 48 such layers and has a total thickness of $\simeq 7\lambda_{\text{int}}$. Light read-out is provided by Bicron WLS-fibers BCF91a with diameter of 1 mm, embedded in round grooves in the scintillator plates. The WLS-fibers from each cell are collected together in a single optical connector at the side of the module. Each of the 9 optical connectors per module at the side of the module is read-out by a single photomultiplier. The 9 PMTs per module are placed at the side of the module with the front-end-electronics.

The short summary of hadron calorimeter's characteristics is presented in Table 1.

5 Straw chamber

Straw detectors arranged in 4 stations and serve to register the tracks of charged particles. The first 2 stations SC1 and SC2 are set before the magnet and contain 6 mm straw-tubes. The other two stations SC3 and SC4 are located after the magnet contain 2 mm straw. Each straw station has sensitive area with dimensions of $200 \times 200 \text{ mm}^2$, and consists of two orthogonal layers.

The gas mixture is usually chosen by the most rapid rate of drift. It is Argon and 20% CO_2 with 2% oxygen – electronegative addition to improve stable operation without disruptions.

The short summary of straw chamber’s characteristics is presented in Table 1.

6 Sc counters, Veto counters and Sc hodoscopes

The main task of these system(S0, S1, S2, V0, V1, H1, H2) is to measure precisely the time of arrival of particles in order to allow the matching with hits detected in the S1 and S2 and to reject pile-up events. The electron tracks were measured by scintillating fiber hodoscopes, arranged upstream and downstream of the magnet. The thickness of the hodoscope planes is of order 3 mm. This is the thickness seen by the beam electrons which will produce bremsstrahlung photons and e^+e^- pairs, and has to be kept as low as possible, compatible with the proposed performance of this sub-detector.

Some more information see Table 1.

7 BGO

The inorganic BGO crystal with a high light yield is used for detection of the SR photons. The crystal were arranged into the 2x4 matrix. Each crystal has hexagonal shape with the diameter of 61 mm and 200 mm long and was viewed by EMI PMT 9603. Electrons with the energy $\lesssim 10 \text{ GeV}$ will be deflected by the magnet at an angle which is larger than those for 100 GeV e^- , and, hence do not hit the ECAL. However, low energy electrons could appear in the beam after the magnet due to the muon $\mu \rightarrow e\nu\nu$ or pion $\pi \rightarrow e\nu$ decays in flight. Since muons and pions do not emit SR photons with energy above the cut, this source of background will also be suppressed.

8 Summary

Table 1: Main characteristics of sub-detectors used in the experiment

ECAL+Preshower	
purpose	energy measurements, shower profile measurements, e/π separation
geometrical dimensions	$\sim 230 \times 230 \times 450 \text{ mm}^3$
weight	$\sim 230 \text{ kg}$
it's a matrix of 6×6 cells, each with dimensions	$38.2 \times 38.2 \times 450 \text{ mm}^3$
number of layers (each layer is 1.50 mm Pb + 1.50 mm Sc)	150 layers or 40 radiation length (X_0), or 1.56 nuclear interaction length
Preshower section	16 layers($\sim 4.27 X_0$)
ECAL section	134 layers($\sim 35.73 X_0$)
energy resolution	$\Delta E/E \simeq 0.09/\sqrt{E} + 0.01$
X,Y resolution	$\simeq 1 \text{ mm}$
e/π	$\lesssim 10^{-2}$
event rate: up to	$\sim 10^7 \text{ e}^-$ per spill, $10^{12} - 10^{13} \text{ e}^-$ in total run
HCAL module	
purpose	secondary energy detection(π, p, n)
number of modules	4
geometrical dimensions	$\sim 600 \times 600 \times 1536 \text{ mm}^3$
weight	$\sim 3500 \text{ kg}$
energy range	$0.5 \div 120 \text{ GeV}$
energy resolution	$\Delta E/E \simeq 0.62/\sqrt{E}$
number of ph. e. produced by MIP in module	$\simeq 150 - 250 \text{ ph. e}$
π -hermeticity	$\simeq 10^{-9}$
Nuclear interaction length	$\approx 7\lambda$
no crack, uniformity	$2 \div 3\%$
number of layers (each layer is 25 mm Fe + 4 mm Sc)	48
length of layer (25 mm Fe + 9 mm gap)	34 mm
number cells per modules	9
cell size	$192 \times 194 \text{ mm}^2$
WLS fiber	BCF91a, 1 mm diameter
read out	PMT(FEU - 84 - 3)
event rate	up to 10^7 e^- per spill
Straw chamber	
purpose	e^- track measurement
number of chambers	4
dimensions of sensitive area	$200 \times 200 \text{ mm}^2$
used gas composition	Ar - 78 %, CO ₂ - 20 %, O ₂ - 2 %
anode signal wire	$20 \mu\text{m}$
kapton(multilayer polyimide film) cathode	$50 \mu\text{m}$
2mm Straw Radiation length	$2.1 \times 10^{-3} X_0$
2mm Straw Nuclear interaction length	$0.94 \times 10^{-3} \lambda_I$
6mm Straw Radiation length	$3.5 \times 10^{-3} X_0$
6mm Straw Nuclear interaction length	$1.45 \times 10^{-3} \lambda_I$

working voltage point for 2 mm straw(gas gain $5 \cdot 10^5$)	1180 V
working voltage point for 6 mm straw(gas gain $5 \cdot 10^5$)	1630 V
operation plateau	$\simeq 200$ V
drift velocity	20 – 30 mm/us
electron collection time for 2 mm straw	$\simeq 25$ ns
electron collection time for 6 mm straw	$\simeq 80$ ns
expected efficiency for one layer of straw for single 2 mm straw	~ 60 %
momentum resolution 100 GeV	$\Delta P/P \simeq 2$ %
Beam counters S0, S1 and hodoscopes H1, H2	
purpose	e^-e^+ pair hits, track detection and T_0
S1 diameter	42 mm
S1 Sc layer thickness	3 mm
S1 Radiation length	$7.75 \times 10^{-3}X_0$
S1 Nuclear interaction length	$4.15 \times 10^{-3}\lambda_I$
S2 diameter	35 mm
S2 Sc layer thickness	3 mm
S2 Radiation length	$7.75 \times 10^{-3}X_0$
S2 Nuclear interaction length	$4.15 \times 10^{-3}\lambda_I$
S3 Diameter	32 mm
S3 Sc layer thickness	5 mm
S3 Radiation length	$1.26 \times 10^{-2}X_0$
S3 Nuclear interaction length	$6.75 \times 10^{-3}\lambda_I$
Veto hole diameter	40 mm
Veto Radiation length	$4.84 \times 10^{-4}X_0$
Veto Nuclear interaction length	$2.6 \times 10^{-4}\lambda_I$
Hodoscope Sc layer thickness	3 mm
Hodoscope Radiation length	$2.9 \times 10^{-2}X_0$
Hodoscope Nuclear interaction length	$1.56 \times 10^{-2}\lambda_I$
spatial resolution	$\simeq 1$ mm
2 tracks separation ΔR	$\gtrsim 3$ mm
event rate	up to 10^6 per spill
Decay volume	
purpose	minimize secondary particles interactions
diameter	$\simeq 26$ cm
length	15 m
wall thickness	6mm Al($6.74 \times 10^{-2}X_0$, $1.51 \times 10^{-2}\lambda_I$)
filling	He or vacuum $\lesssim 10^{-5}$ Torr
Veto counter	
purpose	low energy charged track detection
geometrical dimensions	$55 \times 55 \times 5$ cm ³
mip inefficiency	$\lesssim 10^{-3}$
event rate	up to 10^5 hits per spill
BGO array	
purpose	γ – ray energy measurements in the range 1 – 100 MeV
crystal diameter	61 mm
crystal length	200 mm
thick	200 mm

energy resolution	$\Delta E/E \simeq 3\%$ at 1 Mev
time resolution	$\simeq 2$ ns
event rate (1–30 MeV)	up to 10^6 γ per spill $\simeq 10^{11}$ for full run
read out	EMI PMT 9603
Micromegas tracker	
purpose	e^- track measurement
Radiation length	$1.72 \times 10^{-2} X_0$
Nuclear interaction length	1.9×10^{-3}
number of chambers	4
diameter	80 mm
momentum resolution at 100 GeV	$\Delta P/P \simeq 2\%$
spatial resolution XY	$\simeq 100 \mu m$
event rate	$\sim 10^5 e^-$ per spill